Int J Clin Exp Pathol 2014;7(7):3865-3875
www.ijcep.com /ISSN:1936-2625/IJCEP0000596

Original Article

Unclassified renal cell carcinoma: a clinicopathological, comparative genomic hybridization, and whole-genome exon sequencing study

Zhen-Yan Hu[1*], Li-Juan Pang[1*], Yan Qi[1,2], Xue-Ling Kang[1], Jian-Ming Hu[1,2], Lianghai Wang[1], Kun-Peng Liu[1], Yuan Ren[1], Mei Cui[1], Li-Li Song[1], Hong-An Li[1], Hong Zou[1,2], Feng Li[1]

[1]Department of Pathology, School of Medicine, Shihezi University, Key Laboratory of Xinjiang Endemic and Ethnic Diseases, Ministry of Education of China, Xinjiang 832002, China; [2]Tongji Hospital Cancer Center, Tongji Medical College, Huazhong University of Science and Technology, Wuhan, Hubei, China. [*]Equal contributors.

Received April 22, 2014; Accepted June 2, 2014; Epub June 15, 2014; Published July 1, 2014

Abstract: Unclassified renal cell carcinoma (URCC) is a rare variant of RCC, accounting for only 3-5% of all cases. Studies on the molecular genetics of URCC are limited, and hence, we report on 2 cases of URCC analyzed using comparative genome hybridization (CGH) and the genome-wide human exon GeneChip technique to identify the genomic alterations of URCC. Both URCC patients (mean age, 72 years) presented at an advanced stage and died within 30 months post-surgery. Histologically, the URCCs were composed of undifferentiated, multinucleated, giant cells with eosinophilic cytoplasm. Immunostaining revealed that both URCC cases had strong p53 protein expression and partial expression of cluster of differentiation-10 and cytokeratin. The CGH profiles showed chromosomal imbalances in both URCC cases: gains were observed in chromosomes 1p11-12, 1q12-13, 2q20-23, 3q22-23, 8p12, and 16q11-15, whereas losses were detected on chromosomes 1q22-23, 3p12-22, 5p30-ter, 6p, 11q, 16q18-22, 17p12-14, and 20p. Compared with 18 normal renal tissues, 40 mutated genes were detected in the URCC tissues, including 32 missense and 8 silent mutations. Functional enrichment analysis revealed that the missense mutation genes were involved in 11 different biological processes and pathways, including cell cycle regulation, lipid localization and transport, neuropeptide signaling, organic ether metabolism, and ATP-binding cassette transporter signaling. Our findings indicate that URCC may be a highly aggressive cancer, and the genetic alterations identified herein may provide clues regarding the tumorigenesis of URCC and serve as a basis for the development of targeted therapies against URCC in the future.

Keywords: Unclassified renal cell carcinoma, comparative genomic hybridization, exon GeneChip, chromosome imbalance, gene mutation

Introduction

Unclassified renal cell carcinomas (URCCs) are a group of RCCs with a morphology and/or growth pattern that does not exactly correspond to those of the RCC subtypes recognized by the latest World Health Organization (WHO) classification [1]. Features of URCC include composites of recognized subtypes, mucin production, rare mixtures of epithelial and stromal elements, pure sarcomatoid morphology without recognizable epithelial elements, and unrecognizable cell types. URCCs are rare, accounting for only approximately 3-5% of all RCC cases [2-10]. Most studies on URCC have suggested that this category is associated with unfavorable histological features and aggressive behavior [1, 5, 10, 11].

However, to our knowledge, there are no previous studies on the molecular genetics of URCC, and thus, we describe our experience with 2 cases of URCC analyzed using comparative genome hybridization (CGH) and the genome-wide human exon GeneChip technique to identify genomic alterations characteristic of URCC.

Material and methods

Specimens

Paraffin-embedded tissues (two cases of URCC and 18 cases of normal kidney tissues) were

obtained from the archives of the Department of Pathology, Shihezi University School of Medicine. The clinicopathological data for these cases were collected from the patients' medical records after obtaining permission from the patients and the Institutional Research Ethics Committee. Tumor stages were classified according to the 2004 WHO Classification of the Renal Tumors of the Adults and the 2010 American Joint Committee on Cancer and International Union against cancer tumor/lymph node metastasis/distal metastasis (TNM) classification systems.

Immunohistochemistry (IHC)

The paraffin-embedded tissue sections were stained using the 2-step Envision technique (Dako, Denmark), with primary antibodies against cluster of differentiation (CD)10 (GT-200410, 1:100), cytokeratin (CK) (AE1/AE3, 1:100), vimentin (Vim3B4, 1:100), CD117 (1:300), alpha-methylacyl-CoA racemase (AMACR), transcription factor E3 (TFE3), epidermal growth factor receptor (EGFR), MDM2, p53, P504s (13H4, 1:100), and CK7 (OV-TL12/30, 1:50) (all from Dako, Denmark), according to the manufacturer's instructions. Briefly, after incubation with the primary antibodies, immunodetection was performed using the 2-step method with diaminobenzidine chromogen as a substrate, followed by counterstaining with hematoxylin.

DNA extraction

Total DNA was extracted from the 2 cases of URCC and 18 cases of normal kidney tissue samples by using a standard phenol/chloroform extraction method. DNA quality was checked on a 1% agarose gel, and the amount of extracted DNA was measured spectrophotometrically at 260 nm (impurity and ratio of DNA to non-DNA were also crosschecked at 280 nm). Extractions were stored at -80°C until they were labeled by nick translation.

Comparative genomic hybridization

CGH was performed according to the manufacturer's protocol (Vysis, Inc., Downers Grove, IL, USA). Briefly, labeling reactions were performed with 1 μg DNA and a nick translation labeling kit (Vysis, Inc.) in a volume of 50 μl containing the following: 0.1 mmol/L of a dNTP pool containing 0.3 mmol/L each of dATP, dGTP and dCTP; 0.1 mmol/L dTTP; 0.2 mmol/L fluorescein isothiocyanate (FITC)-dUTP (for the experimental sample) or cyanine 3 (Cy3)-dUTP (for the 46, XY karyotype); and nick translation buffer and nick translation enzyme. The probe size was determined by separation on a 1% agarose gel. Metaphase slides were denatured at (73°C ± 1°C for 5 min in 70% methanamide/2× SSC and dehydrated in an ethanol series (70%, 85%, and 100%). The hybridization mixture consisted of approximately 200 ng Spectrum Green labeled test DNA and 200 ng Spectrum Red total genomic reference DNA co-precipitated with 10 μg of human Cot-1 DNA (Invitrogen, California, USA) and dissolved in hybridization buffer before hybridization to metaphase chromosomes. The probe mixtures were denatured at 73°C for 5 min and then competitively hybridized to the denatured normal metaphase chromosomes in a humid chamber at 37°C for 3 days. After washing, chromosomes were counterstained with 4',6-diamidino-2-phenylindole-2 HCl (DAPI II; Vysis Inc.) and embedded in an anti-fading agent to reduce photo bleaching. A fluorescence microscope equipped with appropriate filters (DAPI, FITC, and Cy3) was used to visualize the signals. For each hybridization panel, raw images from at least 5 metaphases were captured through a computer driven CCD camera and analyzed with the ISIS image software (Carl Zeiss Inc., Goettingen, Germany). Chromosomes were identified by their DAPI banding patterns. Threshold levels of 1.25 and 0.8 were used to score gains and losses, respectively. High-level amplification was indicated by a ratio greater than 1.5. All centromeres, as well as chromosome p35-36, and the heterochromatic regions of chromosomes Y, 16, 19, and 22 were excluded from further analysis because these regions can yield unreliable hybridization owing to incompletely suppressed repetitive DNA sequences. Positive and negative controls provided comparisons for evaluating hybridization and interpretation of the data. Normal female DNA (labeled green) was used as a negative control and normal male DNA was used for reference (labeled red). The intensity profiles for this experiment were within the threshold values, as determined by image analysis. DNA from the MPE600 cell line (with known genetic aberrations that are easy to detect by comparative genomic hybridization) was used as a positive control (labeled green), and normal male DNA was used as a reference.

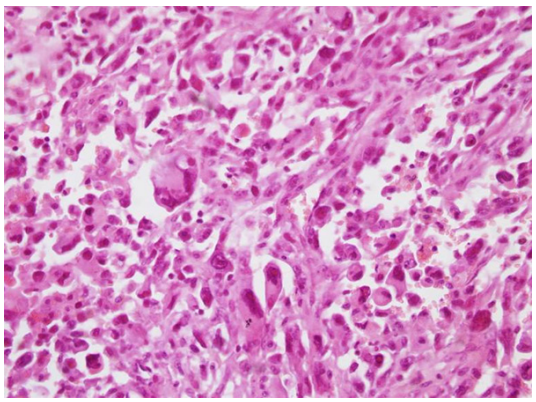

Figure 1. Microscopic findings of URCC. Neoplastic cells intermingled with undifferentiated, round or fusiform multinucleated giant cells with eosinophilic or slightly pale cytoplasm (H&E, × 200).

Human exon GeneChip

A total of 1 μg of DNA from each of the 2 URCC tissues and 18 normal kidney tissues were labeled with Illumina reagents and hybridized to Human Exome BeadChips (Illumina, USA). Illumina Expression Console software was used to perform the quality assessment. The significance analysis of microarrays (SAM) algorithm was used to identify mutated genes in URCC by comparing them with those of normal renal tissues. Gene Ontology biological process enrichment of the classification analysis was used to identify mutated genes associated with cell cycle regulation and other biological functions. The Kyoto Encyclopedia of Genes and Genomes database was used to identify the pathways associated with URCC.

Statistical analysis

The Fisher's exact test was used to compare the differences between the 2 groups (URCC and normal renal tissue). Gene function analysis (Gene Ontology of Biological Processes, Molecular function) was performed by classification enrichment of the gene function and pathways using the Database for Annotation, Visualization, and Integrated Discovery. *P* values < 0.05 were considered statistically significant.

Results

Clinical features

In our study, we analyzed 2 cases of URCC, which accounted for only 1.76% of all 114 cases of RCC managed at the Department of Pathology, Shihezi University School of Medicine, between 1980 and 2013. The male to female ratio was 1:1, and the mean age at diagnosis was 72 years (range, 70-74 years). Both patients were diagnosed with stage III URCC. In addition, the patients presented with fever, kidney pain (patient 1), and painless hematuria (patient 2), which are classic symptoms of RCC. Both patients died within 30 months after surgery.

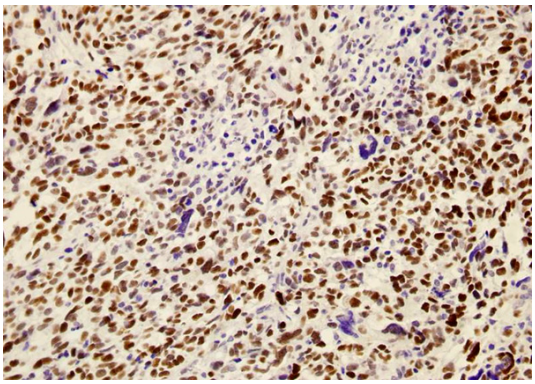

Figure 2. Immunohistochemical findings. URCC shows strong positive expression of p53 (× 200).

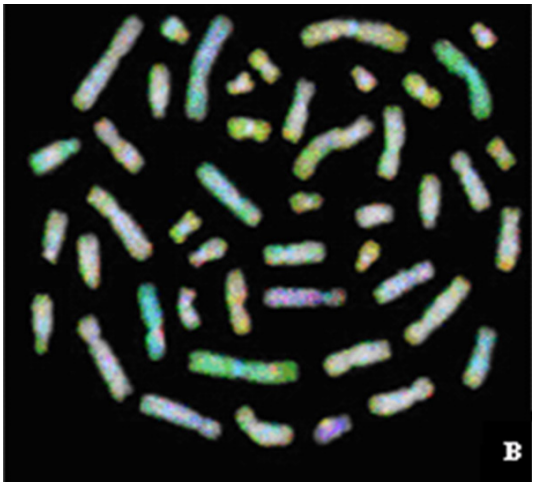

Figure 3. Comparative genomic hybridization profiling of URCCs. Green to red fluorescent thresholds (represented by the green/red line) are 0.8 and 1.25, respectively. Regions of the red indicate loss, regions of the green indicate gains.

Histopathology

The morphology of the 2 URCC cases did not fit into the classifications of any of the known RCC

Table 1. Chromosome aberrations in 2 cases of unclassified renal cell carcinomas (URCCs)

Number	Gain	Loss
URCC 1	1p11, 1q13, 2q20, 3p16, 3q22, 8p12, 10q12-13, 16q11-15	1p28-ter, 1q22, 1q24, 2p28, 2q11, 3p12, 5p30-ter, 6p, 11q, 16q22, 17p13-14, 17q32, 20p
URCC 2	1p12, 1q12-13, 2q23, 3q23, 8p12, 16q11-13, 17p20, 17p22, Yp13	1p18, 1p30-ter, 1q15-20, 1q23-30, 2p20, 2p28, 2p30-ter, 2q12-21, 3p16, 3p21-22, 3q13, 3q30-34, 4q, 5p32-ter, 5q32-34, 6p, 6q, 11p, 11q, 16p13-14, 16q18-22, 17p12-14, 17q18-20, 18q, 19p, 19q, 20p

Table 2. The 32 genes containing missense mutations detected in the URCC tissues ($P < 0.05$)*

Chr	SNP_name	Alleles	in EXON	Mutation(s)	Gene
1	exm1075667	[T/G]	EXON	Missense_A503S	SLC45A1
1	exm131743	[T/C]	EXON	Missense_G68R	C1orf116
1	exm1252046	[T/C]	EXON	Missense_H382Y	CAMSAP2
1	exm1074687	[A/G]	EXON	Missense_L7S	FCRL5
1	exm1162265	[C/G]	EXON	Missense_P935A	PRRC2C
12	exm-rs6584283	[A/G]	EXON	Missense_G83R	ATF1
12	exm-rs9313296	[T/C]	EXON	Missense_R1993W	LRP1
12	exm-rs763469	[T/C]	EXON	Missense_R694Q	ITGA5
12	exm-rs7843884	[A/G]	EXON	Missense_S135N	OR6C4
13	exm1045891	[A/G]	EXON	Missense_I358T	ANKRD10
14	exm1068313	[A/G]	EXON	Missense_G291R	AKAP5
16	exm1147209	[T/G]	EXON	Missense_D191Y	OR2C1
16	exm1176926	[T/C]	EXON	Missense_Q106R,Missense_Q251R	PMFBP1
16	exm1142657	[T/C]	EXON	Missense_T180M	NUBP2
16	exm1187523	[A/G]	EXON	Missense_T297M,	ANKRD11
17	exm1259888	[T/C]	EXON	Missense_K559R,	SLC38A10
17	exm1248013	[T/C]	EXON	Missense_R233W	KIF19
17	exm1256693	[T/C]	EXON	Missense_R574C	ENGASE
17	exm1261710	[T/C]	EXON	Missense_T648M	FOXK2
17	exm1244992	[T/C]	EXON	Missense_V1557A	BPTF
18	exm1263771	[A/G]	EXON	Missense_P842S	LAMA1
19	exm1369588	[A/G]	EXON	Missense_H208Y	C19orf18
19	exm1357108	[A/T]	EXON	Missense_L115M	ZNF480
19	exm1340550	[T/C]	EXON	Missense_R105Q	PLAUR
19	exm1347698	[A/G]	EXON	Missense_R224Q	GLTSCR2
19	exm1309194	[A/G]	EXON	Missense_R240W	MAN2B1
19	exm1327963	[A/G]	EXON	Missense_R295H	MLL4
19	exm128590	[A/G]	EXON	Missense_V102I	AMH
19	exm132178	[T/C]	EXON	Missense_R215Q	PBX4
20	exm1403971	[A/G]	EXON	Missense_R104C	NKAIN4
20	exm1380687	[A/G]	EXON	Missense_R1258C	NINL
20	exm1401664	[T/C]	EXON	Missense_R2351Q	LAMA5

*Fisher's exact test, P value for the comparison between the URCC group and the normal renal tissue group < 0.05.

histological subtypes. The median tumor diameter was 5 cm (range, 2-8 cm). Nodal metastases were identified in 1 case upon evaluation of the perirenal lymph nodes. Grossly, the tumors were solitary, and the cut surface appeared grayish-red, with parts showing necrotic bleeding, resembling rotten fish specimens. The tumors showed a nested and alveolar architecture, and the histological findings included a patchy distribution of undifferentiated, round or

Table 3. Functional enrichment analysis of mutated genes in URCC

Category	Cluster	Term	Count	%	*p* value	Genes
GOTERM_BP_FAT	Cell cycle process, regulation of mitosis	GO:0010564~regulation of cell cycle process	5	4.273504	0.006225	CUL7, CYP1A1, CENPF, RB1, TPR
GOTERM_BP_FAT		GO:0010948~negative regulation of cell cycle process	3	2.564103	0.011143	CENPF, RB1, TPR
GOTERM_BP_FAT		GO:0030071~regulation of mitotic metaphase/anaphase transition	3	2.564103	0.008687	CUL7, CENPF, TPR
GOTERM_BP_FAT		GO:0007346~regulation of mitotic cell cycle	5	4.273504	0.016603	CUL7, CYP1A1, CENPF, RB1, TPR
GOTERM_BP_FAT	Lipid transport, localization	GO:0006869~lipid transport	5	4.273504	0.014192	APOB, ABCG5, NMUR2, ATP10A, ATP8B3
GOTERM_BP_FAT		GO:0010876~lipid localization	5	4.273504	0.018473	APOB, ABCG5, NMUR2, ATP10A, ATP8B3
GOTERM_BP_FAT		GO:0007218~neuropeptide signaling pathway	4	3.418803	0.022012	NMUR2, GPR64, CELSR2, PKD1L2
GOTERM_BP_FAT		GO:0051383~kinetochore organization	2	1.709402	0.02548	CENPF, CENPH
GOTERM_BP_FAT		GO:0051345~positive regulation of hydrolase activity	5	4.273504	0.028229	C5AR1, C9, NMUR2, MYBPC3, DIABLO
GOTERM_BP_FAT		GO:0018904~organic ether metabolic process	3	2.564103	0.0456	APOB, CYP1A1, GPAM
KEGG_PATHWAY		hsa02010:ABC transporters	4	3.418803	0.002295	ABCG5, ABCC4, ABCB5, ABCA6

fusiform multinucleated giant cells with eosinophilic or slightly pale cytoplasm (**Figure 1**).

Immunohistochemical analysis

The IHC analyses of the 2 URCC cases revealed strong positive expression of p53 (**Figure 2**), and partial expression of CD10 and CK. Conversely, staining for CK7, AMACR, CD117, TFE3, EGFR, and MDM2 was negative in both cases, whereas vimentin expression was negative in 1 case and positive in the other.

Comparative genomic hybridization findings

A genomic profile was established based on our set of 2 URCC cases by CGH (**Figure 3**, **Table 1**), with 17 gains and 40 losses identified. High-level losses were observed throughout the whole genome. The chromosomal losses occurred in the following regions: 1p30-ter, 1q24, 2p28, 5p32-ter, 6p, 11q, 16q22, 17p12-14, and 20p. Chromosomal gains occurred in 1p11-12, 1q12-13, 2q20-23, 3q22-23, 8p12, and 16q11-15.

Exon BeadChip

Compared with the 18 normal renal tissues, significant differences in the mutational status of 40 genes ($p < 0.05$) were detected by the exon GeneChip, including 32 missense mutations (**Table 2**) and 8 silent mutations. Functional enrichment analysis revealed that the genes containing missense mutations were involved in 11 different biological processes and pathways ($p < 0.05$), including cell cycle and mitotic metaphase regulation, lipid localization and transport, neuropeptide signaling, organic ether metabolism, and ATP-binding cassette (ABC) transporter signaling (**Table 3**, **Figure 4**).

Discussion

Histological reports of URCC are very rare, with the main sources of information being the 1997 multidisciplinary workshop on renal cell carcinoma and the 2004 WHO pathology classification criteria. URCCs are classified as a subtype of RCC with features that do not fit into any of the other RCC histological subtypes as defined according to the 2004 WHO classification of urological tumors [1]. However, a clear classification of these tumors has not been elucidated, and they appear to display a great diversity in terms of histological and immunohistochemical features. URCC represents 0.7-5.7% of all renal tumors, and most are at a high grade and stage at presentation [10, 12]. While our study confirmed that URCC appears to behave aggressively, its clinical and molecular bases remain to be elucidated.

Histologically, URCCs are frequently composed of a poorly differentiated or predominately sarcomatoid component. To our knowledge, there are currently very few reports regarding the morphological histology of URCC in the literature. In the present study, we found that the 2 analyzed cases of URCC were composed of undifferentiated multinucleated giant cells with eosinophilic cytoplasm, features that do not match those of the other subtypes of RCC.

Immunohistochemically, a great diversity of features have been described for URCC. Zisman et al. [5] reported that URCC stained positive for vimentin and CK, and negative for chromogranin, HMB45 (melanoma-specific antibody), desmin, and muscle-specific actin, and were thus considered to be of epithelial origin. In the present study, both cases of URCC stained strongly positive for p53, with part of the tumor tissues also staining positive for CD10 and CK. Furthermore, one of the tumors also stained positive for vimentin. Positive protein expression of AMACR is a typical feature of papillary renal cell carcinoma, whereas positive CD117 and TFE3 expressions are observed in most chromophobe RCCs and Xp11.2 translocation renal cell carcinomas (Xp11.2 RCCs), respectively, all of which stained negative in the present study. Thus, our immunohistochemical findings were not characteristic of any of the other renal cancer subtypes. However, due to the small sample size in our study, no definite conclusions regarding the immunohistochemical characteristics of URCC can be drawn at the present time.

In addition, a number of recent studies [1, 8, 10, 12] have reported that URCCs are associated with a distinct and highly aggressive biological behavior and poor clinical outcomes compared with other subtypes of RCC. In our study, both patients, classified as having TNM stage III URCC, died, 23 and 30 months post-nephrectomy. However, other studies have

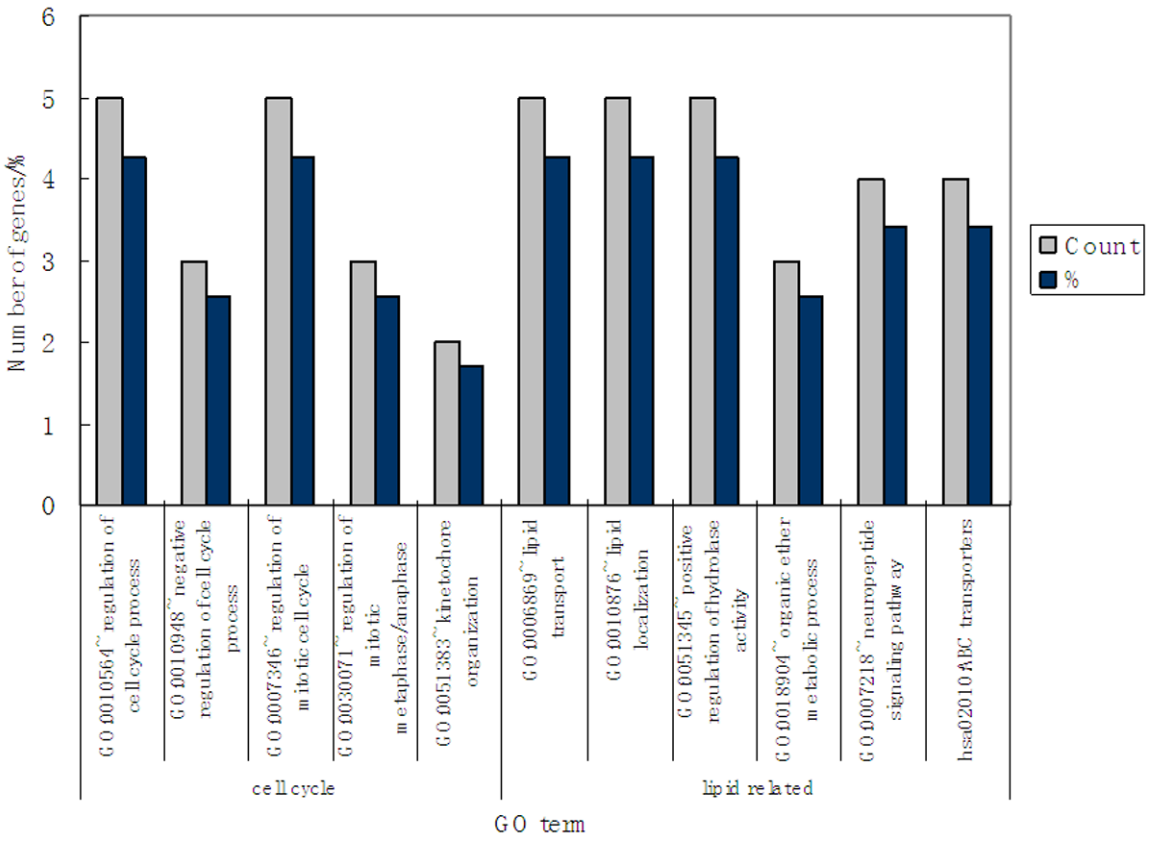

Figure 4. Functional enrichment analysis of URCC mutational status of 40 genes ($P < 0.05$) containing missense mutations detected by the exon GeneChip.

reported that patient survival does not differ significantly between URCC and other subtypes of RCC [7]. The varying outcomes reported in different studies may be related to the definition of URCC. Because there are no specific diagnostic histologic or morphologic features for tumors in this category, it is difficult to know whether the tumors truly belong to the same subtype. This problem could be solved by further molecular genetics studies on the topic, which are currently very limited [7].

In terms of chromosomal events, it has been well established that losses of 3q are associated with the development of clear cell RCC, whereas chromosome 17 gain is a common finding in chromophobe RCC [13]. Moreover, Xp11.2 RCC is characterized by TFE3 gene fusions. In our study, chromosomal losses were observed in chromosomes 1q22-23, 3p12-22, 5p30-ter, 6p, 11q, 16q18-22, 17p12-14, and 20p, whereas gains were observed in chromosomes 1p11-12, 1q12-13, 2q20-23, 3q22-23, 8p12, and 16q11-15 (**Table 1**). These findings did not match the chromosomal events described for any other subtype of RCC.

Interestingly, we found that several of the genes located on the chromosomal regions mentioned above were highly associated with RCC. Seki et al. suggested that roundabout, axon guidance receptor, homolog 1 (ROBO1 [DUTT1], located on 3p12) may be a candidate tumor suppressor gene in RCC [14]. Similarly, He et al. concluded that cell adhesion molecule 2 (located on 3p12) functions as a novel tumor suppressor and may serve as a potential therapeutic target for human RCC [15], whereas Molina et al. reported that fibroblast growth factor receptor 1 (located on 8p12) may represent a potential therapeutic target for the treatment of metastatic RCC [16]. Furthermore, the arachidonate 15-lipoxygenase, type B gene (located on 17p13) has been demonstrated to inhibit

tumor cell proliferation [17], and the reprimo, TP53 dependent G2 arrest mediator candidate gene (located on 2q23) may be involved in the tumorigenicity of RCC [18]. Not only genetic, but also epigenetic, alterations have been described in RCC, with CpG island methylation of hypermethylated in cancer 1 (HIC1, located on 17p13) having been proposed as a candidate marker for improving individualized therapy and risk stratification in RCC. HIC1 is a transcriptional repressor, which functionally cooperates with the p53 tumor suppressor gene, located at 17p13-14 [19].

The p53 gene is known to have numerous important biological functions, including cell cycle regulation, DNA repair, cell differentiation, and apoptosis. p53 protein localizes in the nucleus and functions to combine double chain or single-strand DNA. Numerous studies have shown that mutations of the p53 gene can result in the formation of various tumors, such as endometrial clear cell carcinoma [20]. Accordingly, in this study, the p53 protein overexpression observed in the 2 URCC samples may be associated with the occurrence of URCC, although the exact role of p53 in URCC needs further verification. Based on our findings herein, we conclude that the genes discussed above, which located on the chromosomal regions identified by CGH, are worth further investigation.

To our knowledge, until now, there have been no reports on whole genome sequencing in URCC. For the first time, we used Human Exome BeadChip technology, with the aim to identify mutated genes from 2 cases of URCC as compared with 18 normal renal tissue samples, using the SAM algorithm. Forty mutated genes were detected, distributed on 8 chromosomes, out of which, 32 genes containing missense mutations resulted in exon truncations (**Table 2**). In the functional enrichment analyses, we identified 32 mutated genes, which are known to be involved in 6 different aspects of biological function, including cell cycle regulation, lipid localization and transport, neuropeptide signaling, various metabolic processes, and positive regulation of hydrolase. Among these 32 genes, 16 have been specifically researched in recent years because of their associations with tumorigenesis (**Table 3**). When cell cycle deregulation occurs, cell division, proliferation, differentiation, and apoptosis are consequently affected. We here identified 6 mutated genes associated specifically with the cell cycle and cell cycle regulation (**Table 3**), including cullin-7 (CUL7), centromere protein F (CENPF), and translocated promoter region. Recently, Paradis et al. reported that CUL7 was a novel gene potentially involved in liver carcinogenesis associated with metabolic syndrome, and that amplification of CUL7 resulted in increased cell proliferation [21]. CENPF is used as a marker of cell proliferation in certain human tumors, including lung cancer, liver cancer, and oral squamous cell carcinoma [22-24]. Significant associations between CENPF overexpression and lymph node metastasis and clinical stage have been reported [25], and its expression is associated with mitotic index, as demonstrated by expression of the cell proliferation marker KI-67 [26]. Therefore, overexpression of CENPF may be responsible for the poor cell differentiation and prognosis of URCC, although further verification is needed.

In addition, we here detected that the ABC transporter pathway was associated with URCC. In recent years, ABC, which is a cell membrane protein, has been studied in numerous types of tumors (**Table 3**) and found to play an important role in the development of multiresistant tumors [27, 28]. ABC protein super family members function in the control of efflux pump energy dependence across the cell membrane, and can activate the intracellular to extracellular transport of drugs in order to reduce the concentration of the drug in the cell. Ingram et al. [29] suggested that inhibition of ABC transporters may increase the efficacy of radiation treatment for medulloblastoma patients, and that they are worthy of consideration for the diagnostic classification of these patients. Importantly, Hour et al. [30] reported that ABCD1 downregulation may be involved in human renal tumorigenesis. Therefore, we hypothesize that ABC may cause resistance to effective chemotherapy drugs in URCC, and that inhibition of ABC transporters could increase the efficacy of chemotherapy and radiation treatments.

Furthermore, we here found that functional changes in lipid transport and localization and neuropeptide signaling proteins may be associated with URCC (**Table 3**). In particular, abnor-

mal lipid transport has been demonstrated to correlate with RCC in a number of reports [31-33], with apolipoprotein B being implicated in the development of liver [34], gallbladder [35], breast [36], and kidney cancer [37], among others. In addition, the cadherin, EGF LAG seven-pass G-type receptor 2 has been demonstrated to be an effective target for molecular targeted drugs in breast cancer [38], and in-depth studies of these genes in URCC are warranted.

We found a great deal of consistency in terms of the results from our CGH and exon chip analyses, with some gene exon truncation mutations being found in commonly altered chromosomal regions. For example, chromosomal region 1q23-30 was detected by CGH, and the PRRC2C gene detected by the exon chip is located on 1q23.3. Thus, a combination of CGH and exon chip analyses may facilitate the discovery of mutated genes in not only URCC, but also in other types of cancers.

In conclusion, information regarding genetic alterations in URCC is extremely limited, and the tumorigenesis and clear classification of these tumors have not been fully elucidated. For the first time, we identified a number of chromosomal segments and mutated genes, which may be related to the development of URCC. However, as the sample size was very small, further research on the topic is needed to confirm these results.

Acknowledgements

Supported by grants from the National Natural Science Foundation of China (NSFC, No. 81060209) and from the International S&T Cooperation Program of China (2010DFB-34100).

Disclosure of conflict of interest

None.

Address correspondence to: Dr. Hong Zou, Tongji Hospital Cancer Center, Tongji Medical College, Huazhong University of Science and Technology, Wuhan, Hubei, China; Department of Pathology, School of Medicine, Shihezi University, Xinjiang 832002, China. Tel: 86-13899528366; Fax: 86-0993-2057136; E-mail: zouhong_patho@shzu.edu.cn; Dr. Feng Li, Department of Pathology, School of Medicine, Shihezi University, Xinjiang 832002, China. Tel: 86-13709931299; Fax: 86-0993-2057136; E-mail: lifeng7855@126.com

References

[1] Lopez-Beltran A, Scarpelli M, Montironi R and Kirkali Z. 2004 WHO classification of the renal tumors of the adults. Eur Urol 2006; 49: 798-805.

[2] Senga Y, Taguchi H, Asao T and Misugi K. Undifferentiated renal cell carcinoma in infancy: report of a case and review of literature. Pediatr Pathol 1986; 5: 157-165.

[3] Onishi T, Machida T, Masuda F, Kurauchi H, Suzuki M, Iizuka N and Shirakawa H. [Clinical study of undifferentiated renal cell carcinoma in comparison with well differentiated cases]. Nihon Gan Chiryo Gakkai Shi 1989; 24: 1223-1228.

[4] Ljungberg B, Alamdari FI, Stenling R and Roos G. Prognostic significance of the Heidelberg classification of renal cell carcinoma. Eur Urol 1999; 36: 565-569.

[5] Zisman A, Chao DH, Pantuck AJ, Kim HJ, Wieder JA, Figlin RA, Said JW and Belldegrun AS. Unclassified renal cell carcinoma: clinical features and prognostic impact of a new histological subtype. J Urol 2002; 168: 950-955.

[6] Ficarra V, Schips L, Guille F, Li G, De La Taille A, Prayer Galetti T, Cindolo L, Novara G, Zigeuner RE, Bratti E, Tostain J, Altieri V, Abbou CC, Artibani W and Patard JJ. Multiinstitutional European validation of the 2002 TNM staging system in conventional and papillary localized renal cell carcinoma. Cancer 2005; 104: 968-974.

[7] Crispen PL, Tabidian MR, Allmer C, Lohse CM, Breau RH, Blute ML, Cheville JC and Leibovich BC. Unclassified renal cell carcinoma: impact on survival following nephrectomy. Urology 2010; 76: 580-586.

[8] Lopez-Beltran A, Kirkali Z, Montironi R, Blanca A, Algaba F, Scarpelli M, Yorukoglu K, Hartmann A and Cheng L. Unclassified renal cell carcinoma: a report of 56 cases. BJU Int 2012; 110: 786-793.

[9] Talento R, Hewan-Lowe K and Yin M. Evaluation of morphologically unclassified renal cell carcinoma with electron microscopy and novel renal markers: implications for tumor reclassification. Ultrastruct Pathol 2013; 37: 70-76.

[10] Karakiewicz PI, Hutterer GC, Trinh QD, Pantuck AJ, Klatte T, Lam JS, Guille F, de La Taille A, Novara G, Tostain J, Cindolo L, Ficarra V, Schips L, Zigeuner R, Mulders PF, Chautard D, Lechevallier E, Valeri A, Descotes JL, Lang H, Soulie M, Ferriere JM, Pfister C, Mejean A, Belldegrun AS and Patard JJ. Unclassified renal cell carcinoma: an analysis of 85 cases. BJU Int 2007; 100: 802-808.

[11] Skolarus TA, Serrano MF, Berger DA, Bullock TL, Yan Y, Humphrey PA and Kibel AS. The dis-

tribution of histological subtypes of renal tumors by decade of life using the 2004 WHO classification. J Urol 2008; 179: 439-443; discussion 443-434.
[12] Nakanishi Y, Aihara K, Yo T, Shiraishi Y, Togo Y, Taoka R, Ueda Y, Suzuki T, Higuchi Y, Tsukuda F, Zozumi M, Hirota S, Kanematsu A, Nojima M and Yamamoto S. [Unclassified renal cell carcinoma accompanying pyonephrosis: a case report]. Hinyokika Kiyo 2012; 58: 439-442.
[13] Kallio JP, Mahlamaki EH, Helin H, Karhu R, Kellokumpu-Lehtinen P and Tammela TL. Chromosomal gains and losses detected by comparative genomic hybridization and proliferation activity in renal cell carcinoma. Scand J Urol Nephrol 2004; 38: 225-230.
[14] Seki M, Watanabe A, Enomoto S, Kawamura T, Ito H, Kodama T, Hamakubo T and Aburatani H. Human ROBO1 is cleaved by metalloproteinases and gamma-secretase and migrates to the nucleus in cancer cells. FEBS Lett 2010; 584: 2909-2915.
[15] He W, Li X, Xu S, Ai J, Gong Y, Gregg JL, Guan R, Qiu W, Xin D, Gingrich JR, Guo Y and Chang G. Aberrant methylation and loss of CADM2 tumor suppressor expression is associated with human renal cell carcinoma tumor progression. Biochem Biophys Res Commun 2013; 435: 526-532.
[16] Molina AM, Hutson TE, Larkin J, Gold AM, Wood K, Carter D, Motzer R and Michaelson MD. A phase 1b clinical trial of the multi-targeted tyrosine kinase inhibitor lenvatinib (E7080) in combination with everolimus for treatment of metastatic renal cell carcinoma (RCC). Cancer Chemother Pharmacol 2014; 73: 181-189.
[17] Moussalli MJ, Wu Y, Zuo X, Yang XL, Wistuba II, Raso MG, Morris JS, Bowser JL, Minna JD, Lotan R and Shureiqi I. Mechanistic contribution of ubiquitous 15-lipoxygenase-1 expression loss in cancer cells to terminal cell differentiation evasion. Cancer Prev Res (Phila) 2011; 4: 1961-1972.
[18] Xu M, Knox AJ, Michaelis KA, Kiseljak-Vassiliades K, Kleinschmidt-DeMasters BK, Lillehei KO and Wierman ME. Reprimo (RPRM) is a novel tumor suppressor in pituitary tumors and regulates survival, proliferation, and tumorigenicity. Endocrinology 2012; 153: 2963-2973.
[19] Eggers H, Steffens S, Grosshennig A, Becker JU, Hennenlotter J, Stenzl A, Merseburger AS, Kuczyk MA and Serth J. Prognostic and diagnostic relevance of hypermethylated in cancer 1 (HIC1) CpG island methylation in renal cell carcinoma. Int J Oncol 2012; 40: 1650-1658.
[20] Abe A, Minaguchi T, Ochi H, Onuki M, Okada S, Matsumoto K, Satoh T, Oki A and Yoshikawa H. PIK3CA overexpression is a possible prognostic factor for favorable survival in ovarian clear cell carcinoma. Hum Pathol 2013; 44: 199-207.
[21] Paradis V, Albuquerque M, Mebarki M, Hernandez L, Zalinski S, Quentin S, Belghiti J, Soulier J and Bedossa P. Cullin7: a new gene involved in liver carcinogenesis related to metabolic syndrome. Gut 2013; 62: 911-919.
[22] Clark GM, Allred DC, Hilsenbeck SG, Chamness GC, Osborne CK, Jones D and Lee WH. Mitosin (a new proliferation marker) correlates with clinical outcome in node-negative breast cancer. Cancer Res 1997; 57: 5505-5508.
[23] Liu SC and Klein-Szanto AJ. Markers of proliferation in normal and leukoplakic oral epithelia. Oral Oncol 2000; 36: 145-151.
[24] Zhang JY, Zhu W, Imai H, Kiyosawa K, Chan EK and Tan EM. De-novo humoral immune responses to cancer-associated autoantigens during transition from chronic liver disease to hepatocellular carcinoma. Clin Exp Immunol 2001; 125: 3-9.
[25] Shigeishi H, Mizuta K, Higashikawa K, Yoneda S, Ono S and Kamata N. Correlation of CENP-F gene expression with tumor-proliferating activity in human salivary gland tumors. Oral Oncol 2005; 41: 716-722.
[26] Esguerra RL, Jia L, Kaneko T, Sakamoto K, Okada N and Takagi M. Immunohistochemical analysis of centromere protein F expression in buccal and gingival squamous cell carcinoma. Pathol Int 2004; 54: 82-89.
[27] Ross DD and Nakanishi T. Impact of breast cancer resistance protein on cancer treatment outcomes. Methods Mol Biol 2010; 596: 251-290.
[28] Tang J, Wang Y, Wang D, Wang Y, Xu Z, Racette K and Liu F. Key structure of brij for overcoming multidrug resistance in cancer. Biomacromolecules 2013; 14: 424-430.
[29] Ingram WJ, Crowther LM, Little EB, Freeman R, Harliwong I, Veleva D, Hassall TE, Remke M, Taylor MD and Hallahan AR. ABC transporter activity linked to radiation resistance and molecular subtype in pediatric medulloblastoma. Exp Hematol Oncol 2013; 2: 26.
[30] Hour TC, Kuo YZ, Liu GY, Kang WY, Huang CY, Tsai YC, Wu WJ, Huang SP and Pu YS. Downregulation of ABCD1 in human renal cell carcinoma. Int J Biol Markers 2009; 24: 171-178.
[31] McGuire BB and Fitzpatrick JM. BMI and the risk of renal cell carcinoma. Curr Opin Urol 2011; 21: 356-361.
[32] Gebhard RL, Clayman RV, Prigge WF, Figenshau R, Staley NA, Reesey C and Bear A. Abnormal cholesterol metabolism in renal clear cell carcinoma. J Lipid Res 1987; 28: 1177-1184.
[33] Ericsson JL, Seljelid R and Orrenius S. Comparative light and electron microscopic obser-

vations of the cytoplasmic matrix in renal carcinomas. Virchows Arch Pathol Anat Physiol Klin Med 1966; 341: 204-223.

[34] Cefalu AB, Pirruccello JP, Noto D, Gabriel S, Valenti V, Gupta N, Spina R, Tarugi P, Kathiresan S and Averna MR. A novel APOB mutation identified by exome sequencing cosegregates with steatosis, liver cancer, and hypocholesterolemia. Arterioscler Thromb Vasc Biol 2013; 33: 2021-2025.

[35] Pandey SN, Srivastava A, Dixit M, Choudhuri G and Mittal B. Haplotype analysis of signal peptide (insertion/deletion) and XbaI polymorphisms of the APOB gene in gallbladder cancer. Liver Int 2007; 27: 1008-1015.

[36] Liu X, Wang Y, Qu H, Hou M, Cao W, Ma Z and Wang H. Associations of polymorphisms of rs693 and rs1042031 in apolipoprotein B gene with risk of breast cancer in Chinese. Jpn J Clin Oncol 2013; 43: 362-368.

[37] Van Hemelrijck M, Garmo H, Hammar N, Jungner I, Walldius G, Lambe M and Holmberg L. The interplay between lipid profiles, glucose, BMI and risk of kidney cancer in the Swedish AMORIS study. Int J Cancer 2012; 130: 2118-2128.

[38] Huang H, Groth J, Sossey-Alaoui K, Hawthorn L, Beall S and Geradts J. Aberrant expression of novel and previously described cell membrane markers in human breast cancer cell lines and tumors. Clin Cancer Res 2005; 11: 4357-4364.